Environ Health Perspect
DOI: 10.1289/EHP493

Supplemental Material

Heat-Related Mortality in Japan after the 2011 Fukushima Disaster: An Analysis of Potential Influence of Reduced Electricity Consumption

Yoonhee Kim, Antonio Gasparrini, Masahiro Hashizume, Yasushi Honda, Chris Fook Sheng Ng, and Ben Armstrong

Table of Contents

temperature (B) in Tokyo and daily electricity consumption across the eight prefectures served by the Tokyo Electric Power Company (TEPCO) listed in Table S1. The vertical line indicates the date of the Great East Japan Earthquake occurred on 11 March 2011.

Figure S2. Forest plot for prefecture-specific ratio of relative risks (RRRs) for all-cause mortality associated with heat (the 99th percentile of daily mean temperature during May–September for prefecture specific shown in Table S1) compared with the 50th percentile of the temperature over 0–10 lag days after to before the earthquake and 95% confidence intervals based on the distributed lag non-linear model adjusted for day-of-week or holiday, date, and day-in-season (natural cubic spline with 4 df/year) × year. The periods for before and after correspond to 2008–2010 and 2011–2012, respectively. A fixed effect meta-analysis was used to estimate the summary RRRs in less-affected and most-affected areas.

Figure S3. Prefecture-specific cumulative relative risks (RRs) for all-cause mortality associated with daily mean temperature during May–September for prefecture specific (the distribution of the temperature shown in Table S1) compared with the 50th percentile of the temperature over 0–10 lag days before and after the earthquake and 95% confidence intervals based on the distributed lag non-linear model adjusted for day-of-week or holiday, date, and day-in-season (natural cubic spline with 4 df/year) × year (1st column), their lag-response curves of the RRs for the 95th percentile of daily mean temperature (2nd column), and changes in the RRs after to before (ratio of relative risks, RRRs) (3rd column). The shaded areas indicate 95% confidence intervals.

Figure S4. Cumulative relative risks for all-cause (ALL), cardiovascular (CVD), and respiratory (RESP) mortality for people aged 65 and over associated with heat at the 95th (A) or 99th (B) percentiles of daily mean temperature during May–September in Tokyo (30.1°C or 31.1°C, respectively), compared with those for the 50th percentile of the temperature (24.4°C) over 0–10 lag days, stratified by the estimated percent reduction in electricity consumption (i.e. the difference between observed and expected consumption after the earthquake based on a model adjusted for temperature, day-of-week or holiday, and day-in-season using daily electricity consumption in the TEPCO service area that includes Tokyo).

Figure S5. Results by sensitivity analysis excluding the 2011 data showing forest plot for prefecture-specific ratio of relative risks (RRRs) for all-cause mortality associated with heat (the 95th percentile of daily mean temperature during May–September for prefecture specific shown in Table S1) compared with the 50th percentile of the temperature over 0–10 lag days after to before the earthquake and 95% confidence intervals based on the distributed lag non-linear model adjusted for day-of-week or holiday, date, and day-in-season (natural cubic spline with 4 df/year) × year. The periods for before and after correspond to 2008–2010 and 2011–2012, respectively. A fixed effect meta-analysis was used to estimate the summary RRRs in less-affected and most-affected areas. The results were consistent with the main results although the 95% confidence intervals became wider due to the smaller statistical power.

Figure S6. Results by sensitivity analyses. Estimated ratio of relative risks (RRRs) with 95% confidence intervals (CIs) in Tokyo based on the interrupted time-series analysis, according to increases in (A) degree of piecewise polynomials of B-spline basis for temperature, (B) degree of freedom of the natural cubic spline for day-in-season, (C) the place of knot for the spline of temperature, and (D) the placement of reference temperature. (E) The cumulative relative risks for all-cause mortality associated with daily mean temperature during May–September compared with the 50th percentile of the temperature over 0–21 lag days and (F) their lag-response curves for the 95th percentile of daily mean temperature in Tokyo. The shaded areas in panels (E) and (F) indicate 95% confidence intervals. (G) Deviance residuals over time and (H) partial autocorrelation function based on the final model of interrupted time-series analysis in Tokyo.

Figure S7. Results by sensitivity analyses. The cumulative relative risks for all-cause mortality associated with daily mean temperature during May–September compared with the 50th percentile of the temperature over 0–10 lag days in Tokyo based on the interrupted time-series analysis, applying a range of number of knots for the quadratic B-spline of daily mean temperature from 1 knot to 4 knots. The shaded areas in each panel indicate 95% confidence intervals.

Table S1. Summary statistics of power use, mortality, and daily mean temperature across 47 prefectures in Japan by less- and most-affected areas

Area[a]	Power use[b]	Power Company	Prefecture	Population[c]	The number of deaths[d]				Daily mean temperature[d]			
					All-cause	CVD[e]	Respiratory	65+ (%)[f]	Median	IQR[g]	95th	99th
Less	100	Hokuriku	Fukui	806314	16192	4362	2838	88.4	24.1	7	30	30.6
	100	Hokuriku	Ishikawa	1169788	22354	6038	3487	87	23.7	7.2	29.7	30.4
	100	Hokuriku	Toyama	1093247	23170	6059	3759	87.3	23.5	6.8	29.6	30.5
	98.4	Okinawa	Okinawa	1392818	20661	5156	3447	78.2	28.3	2.9	29.7	30.1
	97.9	Hokkaido	Hokkaido	5506419	111397	30707	16364	84.3	19.7	6.8	25.4	27.1
	97.7	KEPCO	Hyogo	5588133	97816	24479	14711	84.7	25.4	6.2	30	30.6
	97.7	KEPCO	Kyoto	2636092	46227	12203	7181	85.9	25	6.8	30.5	31.2
	97.7	KEPCO	Nara	1400728	24626	6780	3884	86.3	23.9	6.5	29.2	29.8
	97.7	KEPCO	Osaka	8865245	149161	37248	24004	82.7	25.6	6.5	30.7	31.2
	97.7	KEPCO	Shiga	1410777	22063	6030	3353	86.1	24.2	7.1	29.8	30.2
	97.7	KEPCO	Wakayama	1002198	23119	6011	3828	87	25.3	6.1	29.6	30.3
	97.2	Kyuushu	Fukuoka	5071968	90561	21093	15118	84.1	25.1	6.6	30.5	31.3
	97.2	Kyuushu	Kagoshima	1706242	39350	11117	7096	86.8	26.5	5.9	30	30.6
	97.2	Kyuushu	Kumamoto	1817426	37183	9832	6358	87.1	25.8	6.1	30.1	30.8
	97.2	Kyuushu	Miyazaki	1135233	23847	6813	3957	86.1	25.4	5.6	29.2	30.2
	97.2	Kyuushu	Nagasaki	1426779	31360	8208	5455	85.9	25.2	6.2	29.6	30.4
	97.2	Kyuushu	Oita	1196529	25293	6648	4462	87.1	24.9	6.1	29.5	30.2

	97.2	Kyuushu	Saga	849788	17735	4553	3135	86.2	25.2	6.2	30	30.7
	97.1	Shikoku	Ehime	1431493	31153	8794	5167	85.8	25.1	6.3	30	30.5
	97.1	Shikoku	Kagawa	995842	20750	5444	3809	86.7	25.4	6.5	30.6	31.3
	97.1	Shikoku	Kochi	764456	18810	5363	3225	87.1	25.5	5.5	29.4	30
	97.1	Shikoku	Tokushima	785491	17643	4526	3041	87.2	24.9	6.1	29.6	30.4
	96.5	Chuugoku	Hiroshima	2860750	53335	14017	8740	85.9	24.9	6.1	30.3	30.8
	96.5	Chuugoku	Okayama	1945276	38233	10130	7016	87.2	25.3	6.5	30.7	31.3
	96.5	Chuugoku	Shimane	717397	17515	4699	2768	88.8	23.6	6.7	29.5	30.3
	96.5	Chuugoku	Tottori	588667	13167	3630	1803	86.4	23.9	7.1	29.9	30.8
	96.5	Chuugoku	Yamaguchi	1451338	33777	9148	6104	87.5	24.5	6.1	29.6	30
	96.2	Chuubu	Aichi	7410719	111054	27411	16189	83.2	25.1	6.3	30.4	31.3
	96.2	Chuubu	Gifu	2080773	38586	10492	5904	86.4	24.9	6.1	30.5	31.5
	96.2	Chuubu	Mie	1854724	34871	9085	5229	86.4	24.8	6.4	30	31.3
	96.2	Chuubu	Nagano	2152449	44436	13397	6377	88.6	22.3	6.8	27.7	28.4
	96.2	Chuubu	Shizuoka	3765007	68364	18604	9462	85.7	24.5	6	29.2	30
Most	89.1	TEPCO	Chiba	6216289	95768	26787	13973	82.4	24	6.7	29.5	30.2
	89.1	TEPCO	Gunma	2008068	38627	10840	6538	85.3	23.8	6.7	30	30.9
	89.1	TEPCO	Ibaraki	2969770	54385	15032	8245	83.7	22.2	6.8	28.5	29.4
	89.1	TEPCO	Kanagawa	9048331	131393	33868	19286	82.5	24	6.7	29.1	30
	89.1	TEPCO	Saitama	7194556	106417	28749	15613	81.3	24	6.8	30.3	31.2

89.1	TEPCO	Tochigi	2007683	37229	10812	5475	83.9	22.9	6.6	28.9	29.7
89.1	TEPCO	Tokyo	13159388	200030	51957	29365	83.1	24.4	7	30.1	31.1
89.1	TEPCO	Yamanashi	863075	17420	4638	2610	86.8	23.8	6.3	29.1	29.8
89.1	Tohoku	Akita	1085997	27542	7773	4303	87.2	21.7	6.9	28	29
89.1	Tohoku	Aomori	1373339	31586	9115	4553	84.1	20	7	26.9	28.8
89.1	Tohoku	Fukushima	2029064	43006	12948	6389	85.8	22.2	6.9	29.2	30
89.1	Tohoku	Iwate	1330147	30097	9380	4429	86.6	20.7	7	27.1	28.1
89.1	Tohoku	Miyagi	2348165	41413	11901	5768	84.6	21.2	6.8	27.8	29.2
89.1	Tohoku	Niigata	2374450	50654	14562	6857	87.2	23.2	6.6	29.2	30.2
89.1	Tohoku	Yamagata	1168924	27645	7953	4313	88.5	21.8	6.9	28.2	29.2

[a]Prefectures were classified into two groups defined *a priori* as the most affected (>10% reduction in the estimated proportion[b] of power use in 2011 during June–September compared with average power use before the earthquake) and less affected (≤10% reduction in the power use); [b]Estimated proportion of power use in 2011 during June–September for each prefecture compared with average power use in the same prefectures in 2007–2010 obtained from The Federation of Electric Power Companies of Japan; [c]Population census in 2010 obtained from Statistics Bureau, Ministry of Internal Affairs and Communications, Japan (http://www.stat.go.jp/english/data/kokusei, accessed on 11 June, 2015); [d]The distributions of the number of deaths and daily mean temperature were based on the data during May–September (warm season) in 2008–2012; [e]Cardiovascular death; [f]Percentage of all-cause deaths for people aged 65 years and over; [g]Interquartile range.

Table S2. Mean cumulative relative risks and ratio of relative risks with 95% confidence intervals in less-affected and most-affected areas for people aged 65 years and over

Heat[a]	Cause of death	Area	RR[b] before	RR[b] after	RRR[c] after/before	p-value[d]
95%	All-cause	Less	1.03 (1.01, 1.05)	1.04 (1.01, 1.06)	1.01 (0.97, 1.04)	0.007
		Most	1.09 (1.06, 1.12)	1.02 (0.99, 1.05)	0.94 (0.90, 0.97)	
	Cardiovascular	Less	1.06 (1.02, 1.10)	1.04 (0.99, 1.09)	0.98 (0.92, 1.05)	0.906
		Most	1.10 (1.04, 1.16)	1.07 (1.02, 1.12)	0.98 (0.91, 1.05)	
	Respiratory	Less	0.99 (0.95, 1.04)	1.07 (1.01, 1.13)	1.07 (0.99, 1.16)	0.274
		Most	1.07 (0.99, 1.14)	1.06 (1.00, 1.13)	0.98 (0.90, 1.08)	
99%	All-cause	Less	1.04 (1.01, 1.08)	1.08 (1.04, 1.12)	1.03 (0.98, 1.08)	0.001
		Most	1.19 (1.13, 1.24)	1.06 (1.02, 1.10)	0.89 (0.84, 0.95)	
	Cardiovascular	Less	1.10 (1.04, 1.16)	1.08 (1.01, 1.16)	0.99 (0.90, 1.09)	0.353
		Most	1.25 (1.15, 1.37)	1.14 (1.06, 1.22)	0.92 (0.82, 1.03)	
	Respiratory	Less	1.00 (0.93, 1.07)	1.16 (1.07, 1.26)	1.16 (1.03, 1.30)	0.058
		Most	1.16 (1.04, 1.30)	1.13 (1.03, 1.24)	0.95 (0.82, 1.10)	

[a] The 95th and 99th percentiles of daily mean temperature during May–September were defined using prefecture-specific temperature distributions. Cumulative relative risks (RRs[b]) and ratio of relative risks (RRRs[c]) for mortality associated with heat compared with the 50th percentile of temperature during May–September were estimated by a distributed lag non-linear model over 0–10 lag days, adjusted for day-of-week or holiday, date, and day-in-season (natural cubic spline with 4 df/year) × year. The periods for before and after correspond to 2008–2010 and 2011–2012, respectively. A fixed effect meta-analysis was used to combine the prefecture-specific RRs or RRRs in less-affected and most-affected areas with a range of I^2 statistics, 0.0–37.9%, suggesting no evidence of heterogeneity (all of p<0.05 by test for heterogeneity). The most-affected prefectures are the 15 prefectures that reduced electricity consumption by >10% following the earthquake (reported by electric power companies; Table S1) and the less-affected prefectures are the remaining 32 prefectures, specifically listed in Figure 2. [d] Random-effects meta-regression was used to test the difference of RRs or RRRs between most-affected and less-affected areas.

Table S3. Cumulative relative risks (RRs) and the ratio of relative risk (RRRs) for all-cause mortality associated with heat (defined as the 95th percentile of daily mean temperature during May–September) over 0–10 lag days, compared with those for the 50th percentile of the temperature, combined by meta-analysis across 13 prefectures[a] in the most-affected area and 95% confidence intervals, based on the interrupted time-series (ITS) analysis with and without adjustment for an air pollutant (2-days moving average)

Risk estimate	Without adjustment	Adjusted for SPM	Adjusted for NO_2	Adjusted for SO_2	Adjusted for O_3
RR (Before)	1.08 (1.05, 1.11)	1.07 (1.04, 1.10)	1.08 (1.05, 1.11)	1.08 (1.05, 1.11)	1.06 (1.03, 1.09)
RR (After)	1.02 (1.00, 1.05)	1.02 (0.99, 1.05)	1.02 (1.00, 1.05)	1.02 (1.00, 1.05)	1.02 (0.99, 1.05)
RRR (After/Before)	0.95 (0.92, 0.99)	0.95 (0.92, 0.99)	0.95 (0.91, 0.99)	0.95 (0.91, 0.99)	0.96 (0.93, 1.00)

[a] Gunma and Yamanashi were excluded in the analyses for SPM and SO_2 adjustment, respectively, due to incomplete data. The 95th percentiles of daily mean temperature during May–September were defined using prefecture-specific temperature distributions. Cumulative relative risks (RRs) and ratio of relative risks (RRRs) for mortality associated with heat compared with the 50th percentile of temperature during May–September were estimated by a distributed lag non-linear model over 0–10 lag days, adjusted for day-of-week or holiday, date, and day-in-season (natural cubic spline with 4 df/year) × year. The periods for before and after correspond to 2008–2010 and 2011–2012, respectively. A fixed effect meta-analysis was used to combine the prefecture-specific RRs or RRRs in the most-affected areas including the 13 prefectures that reduced electricity consumption by >10% following the earthquake (reported by electric power companies) and that air pollution data available since 2008 (please see the details below).

Data and analyses for Table S3

We obtained hourly data for suspended particulate matter (SPM), nitrogen dioxide (NO_2), sulfur dioxide (SO_2), and ozone (O_3) from the National Institute for Environmental Studies, Japan. SPM refers to air particles collected with an upper 100% cut-off at 10 μm aerodynamic diameter under the air quality standard in Japan. Air pollutant data were available for 13 of the 15 most-affected prefectures for the period May–September, 2008–2012 (Miyagi, Akita, Yamagata, Fukushima, Ibaraki, Tochigi, Gunma, Saitama, Chiba, Tokyo, Kanagawa, Niigata, and Yamanashi). Air pollutants were measured continuously at multiple automated air quality monitoring stations (ranging from 11 to 92 stations per prefecture). For each station, hourly values of SPM, NO_2, and SO_2 were averaged to obtain daily means. For O_3, we computed the daily maximum 8 hour moving averages. To obtain citywide average concentration, we averaged the values from multiple stations, excluding days with more than 5 missing hourly values and stations with 30 or more missing daily values. There was no missing value at the prefecture level, except for Gunma and Yamanashi which had incomplete SPM and SO_2 data, respectively. These two prefectures were selectively excluded from air pollutant adjustment.

We performed a sensitivity analysis to examine if the heat-mortality association was changed by air pollutant by including a 2-day moving average of air pollutant concentration as a linear term in the interrupted time-series (ITS) model described in the main text. Air pollutant variables were included one at a time because some were highly correlated in certain locations.

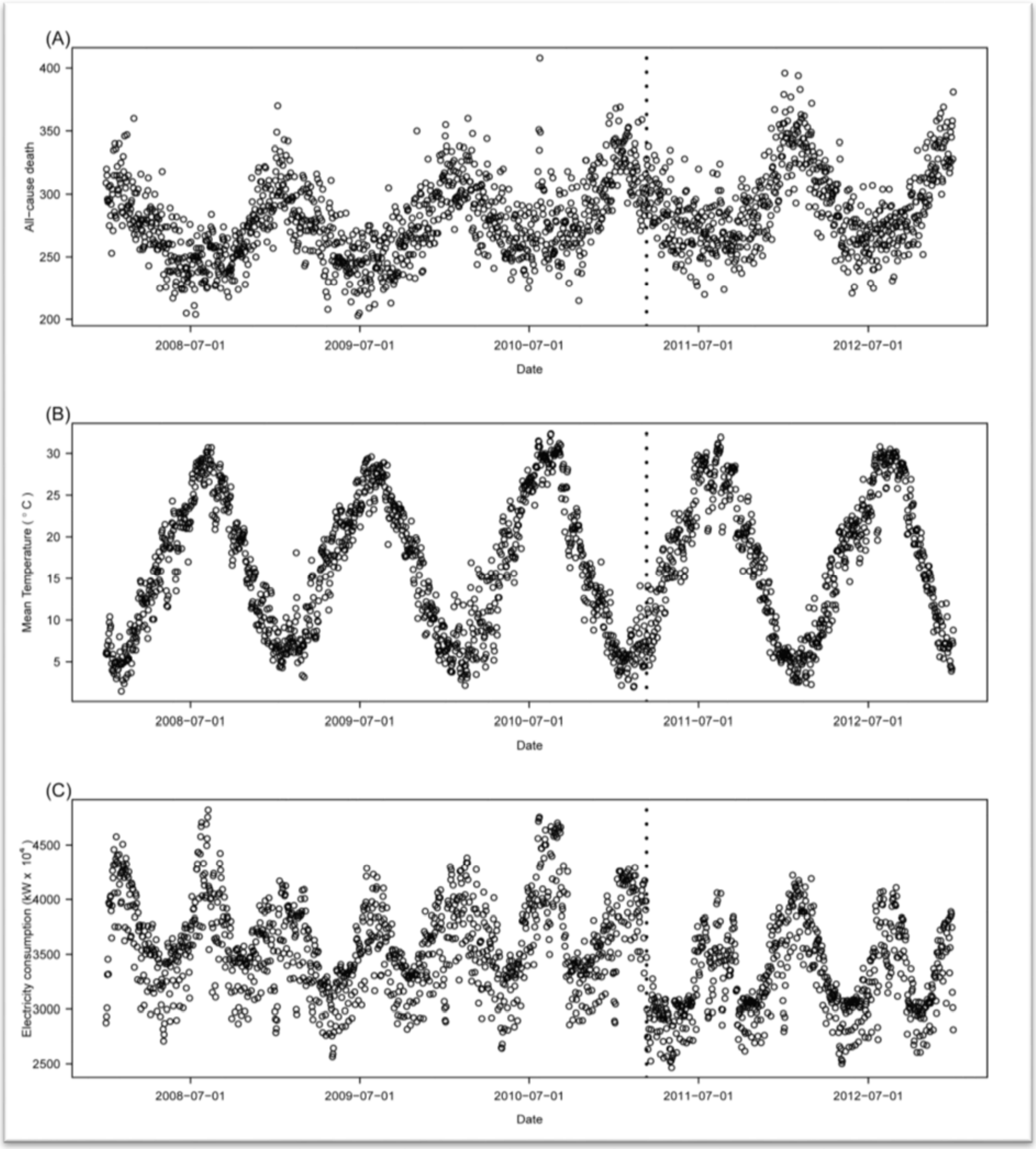

Figure S1. Time-series plots of the daily number of all-cause deaths (A) and daily mean temperature (B) in Tokyo and daily electricity consumption across the eight prefectures served by the Tokyo Electric Power Company (TEPCO) listed in Table S1. The vertical line indicates the date of the Great East Japan Earthquake occurred on 11 March 2011.

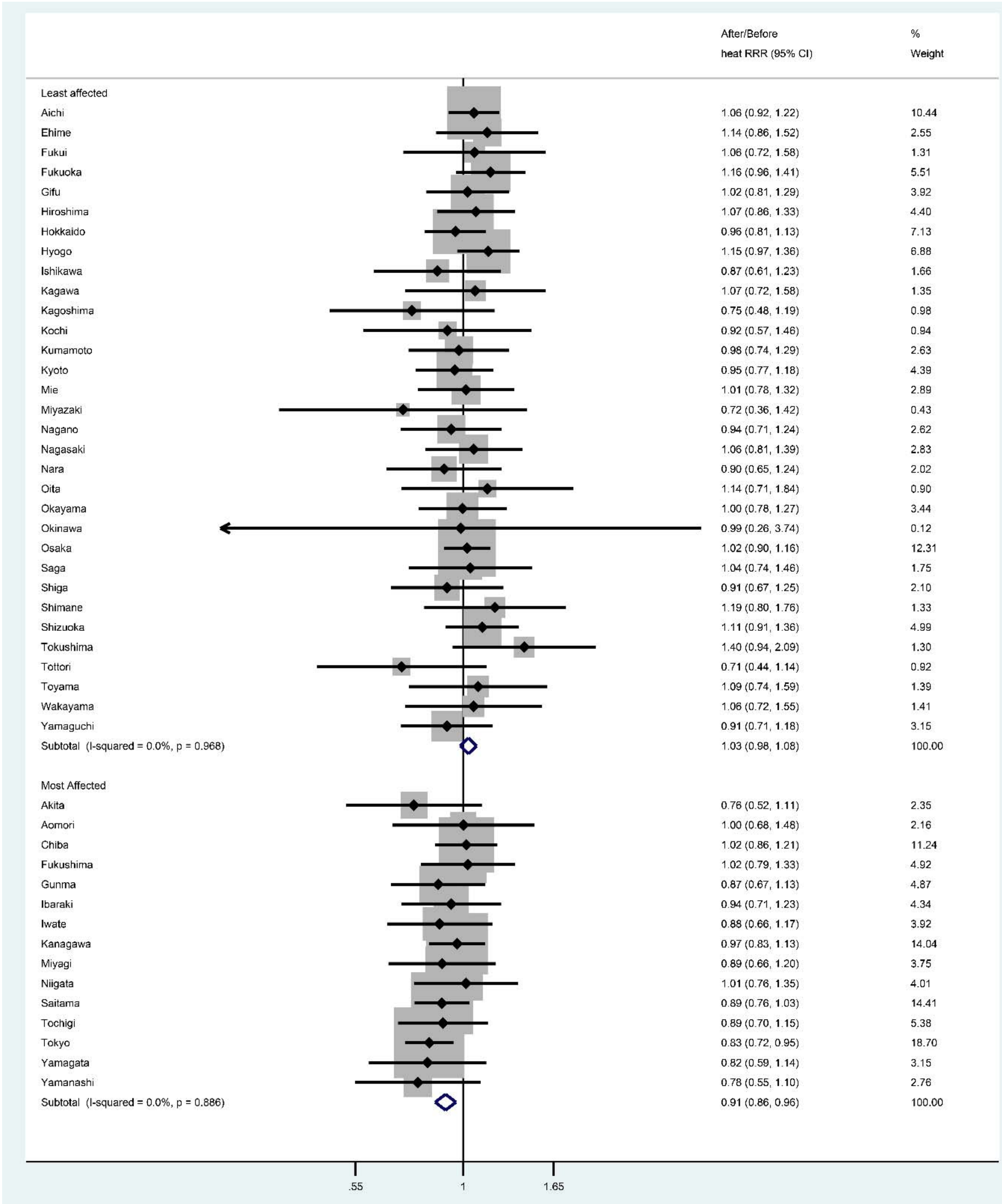

Figure S2. Forest plot for prefecture-specific ratio of relative risks (RRRs) for all-cause mortality associated with heat (the 99th percentile of daily mean temperature during May–September for prefecture specific shown in Table S1) compared with the 50th percentile of the temperature over 0–10 lag days after to before the earthquake and 95% confidence intervals based on the distributed lag non-linear model adjusted for day-of-week or holiday, date, and day-in-season (natural cubic spline with 4 df/year) × year. The periods for before and after correspond to 2008–2010 and 2011–2012, respectively. A fixed effect meta-analysis was used to estimate the summary RRRs in less-affected and most-affected areas.

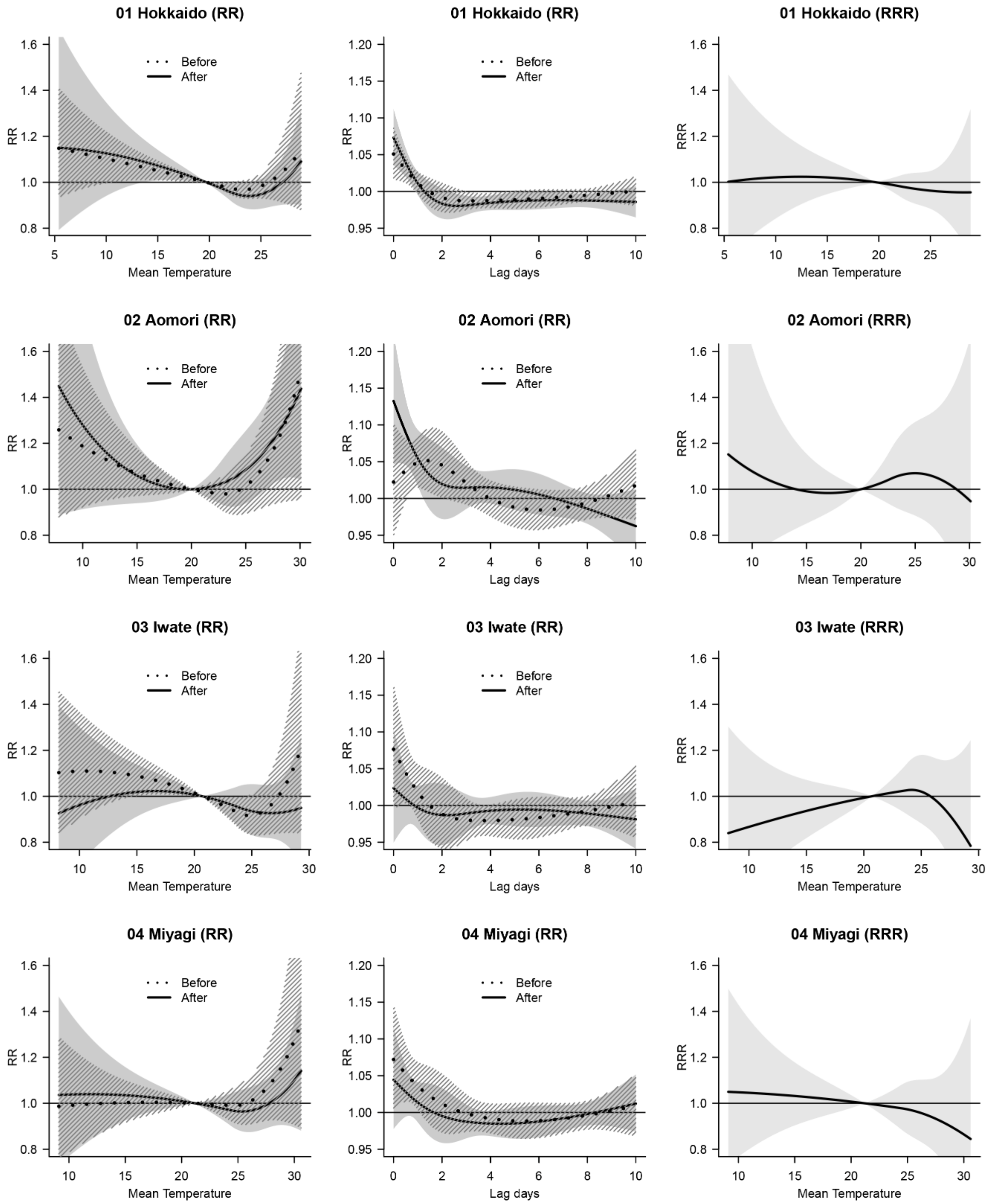
01 Hokkaido (RR)
01 Hokkaido (RR)
01 Hokkaido (RRR)
02 Aomori (RR)
02 Aomori (RR)
02 Aomori (RRR)
03 Iwate (RR)
03 Iwate (RR)
03 Iwate (RRR)
04 Miyagi (RR)
04 Miyagi (RR)
04 Miyagi (RRR)
Before
After
RR
RRR
Mean Temperature
Lag days

Figure S3. Prefecture-specific cumulative relative risks (RRs) for all-cause mortality associated with daily mean temperature during May–September for prefecture specific (the distribution of the temperature shown in Table S1) compared with the 50th percentile of the temperature over 0–10 lag days before and after the earthquake and 95% confidence intervals based on the distributed lag non-linear model adjusted for day-of-week or holiday, date, and day-in-season (natural cubic spline with 4 df/year) × year (1st column), their lag-response curves of the RRs for the 95th percentile of daily mean temperature (2nd column), and changes in the RRs after to before (ratio of relative risks, RRRs) (3rd column). The shaded areas indicate 95% confidence intervals.

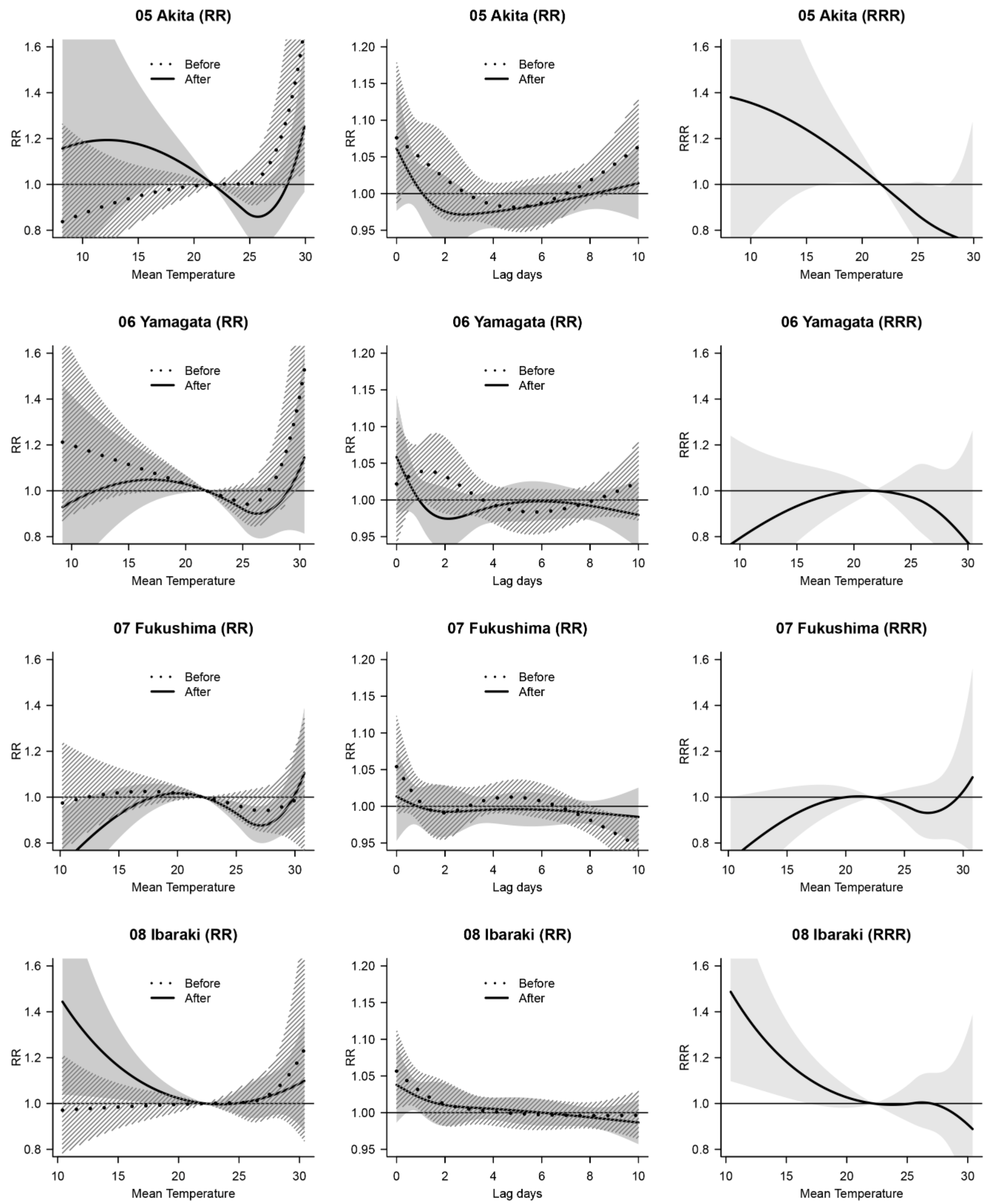

Figure S3. Continued.

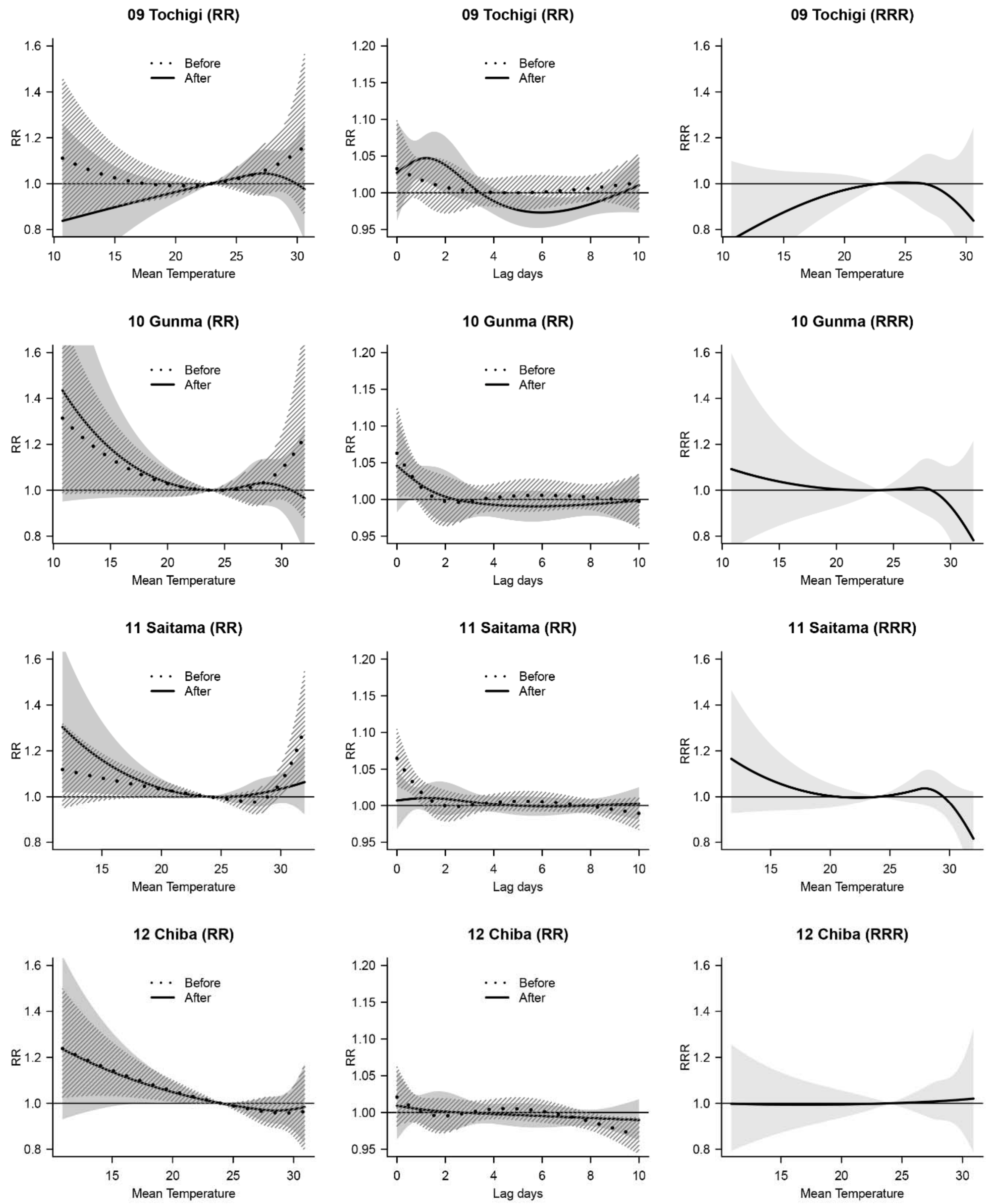

Figure S3. Continued.

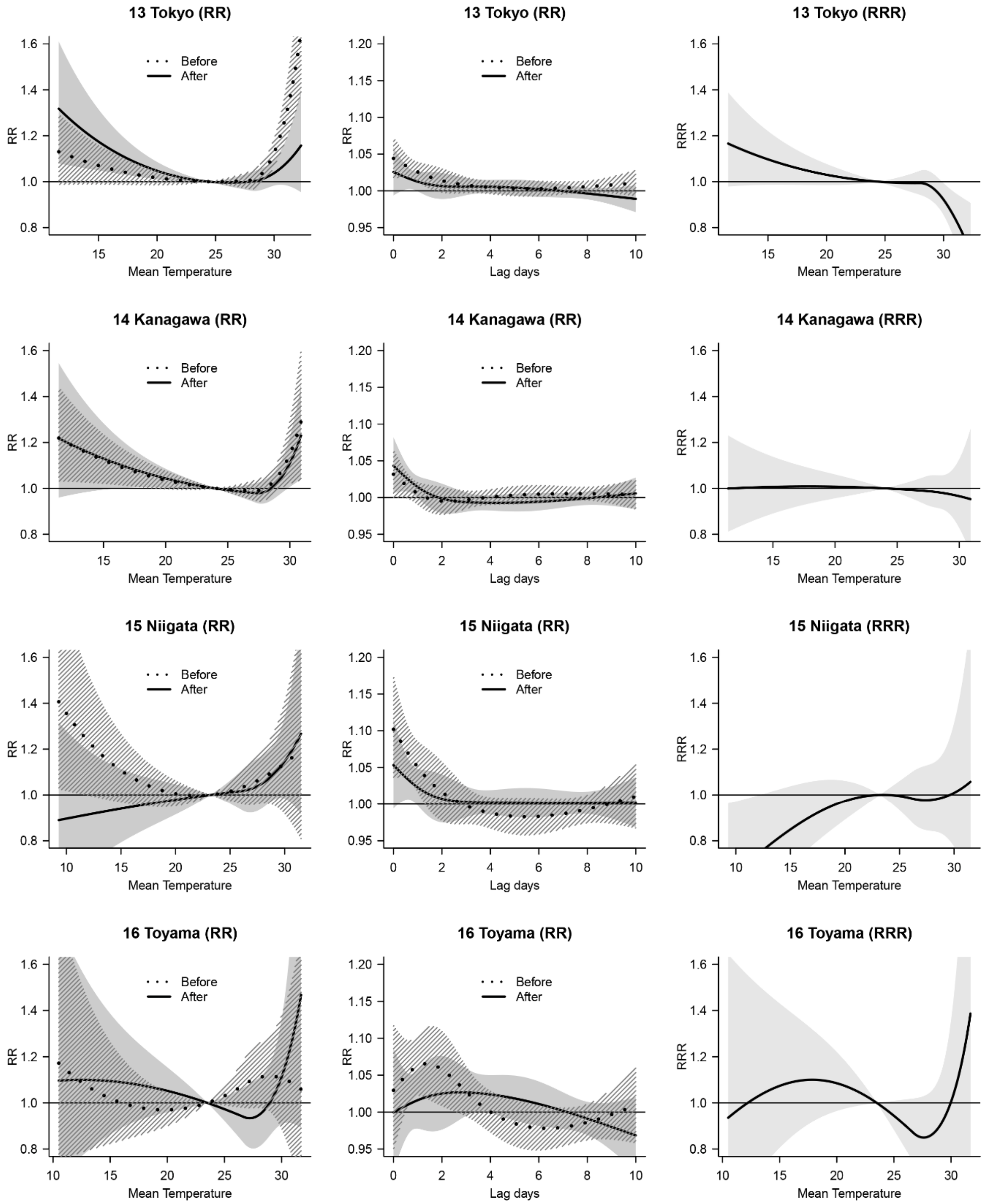

Figure S3. Continued.

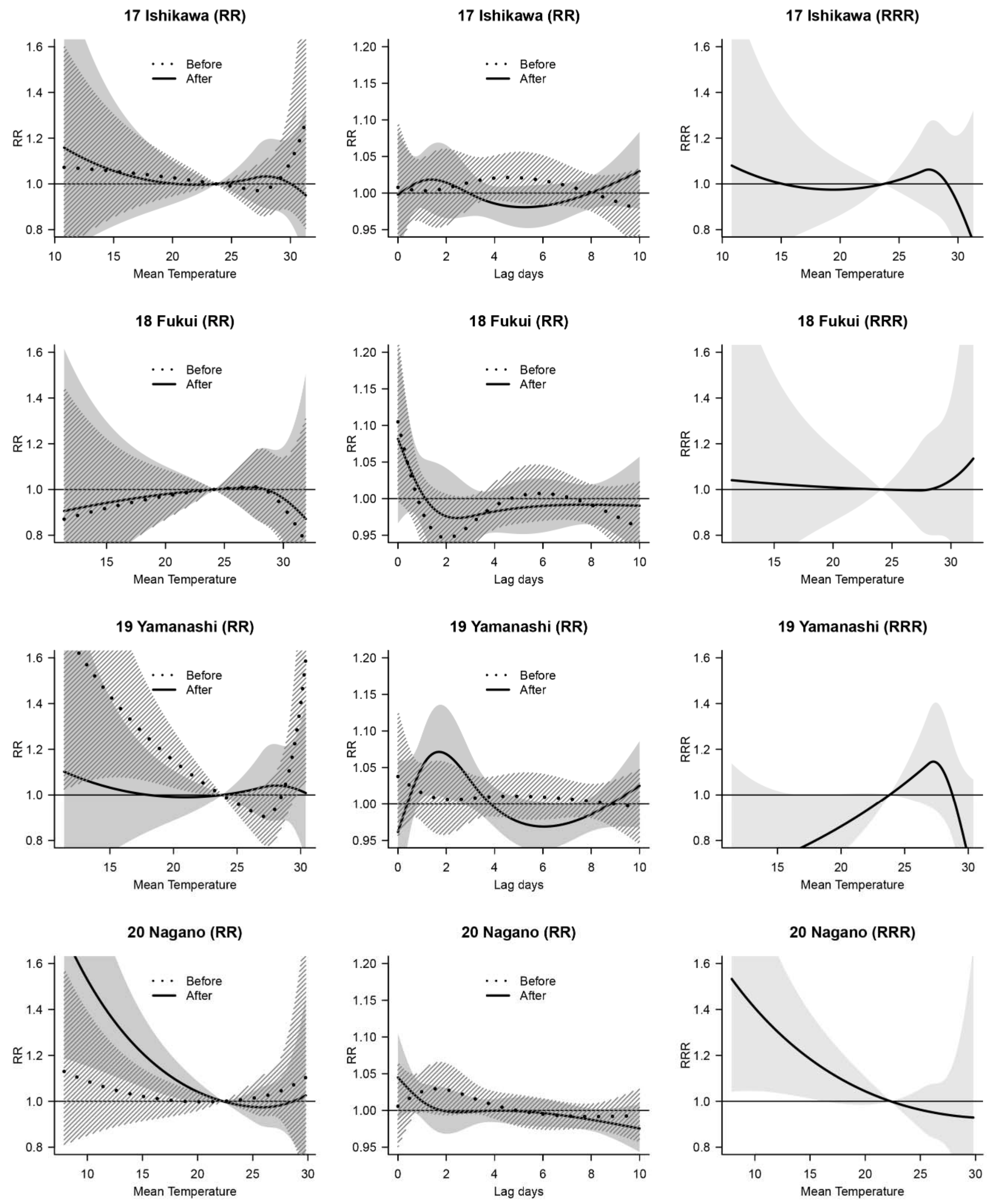

Figure S3. Continued.

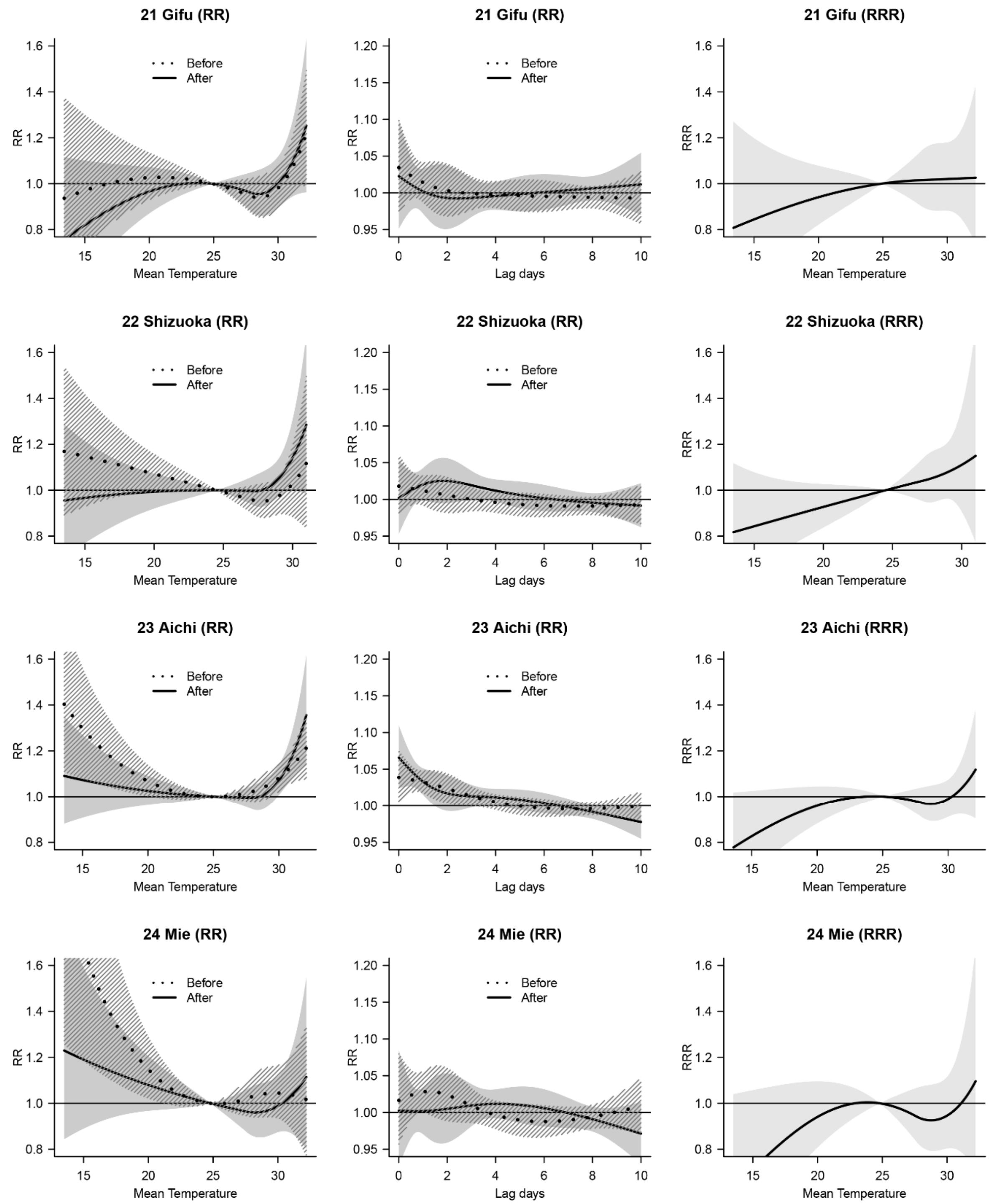

Figure S3. Continued.

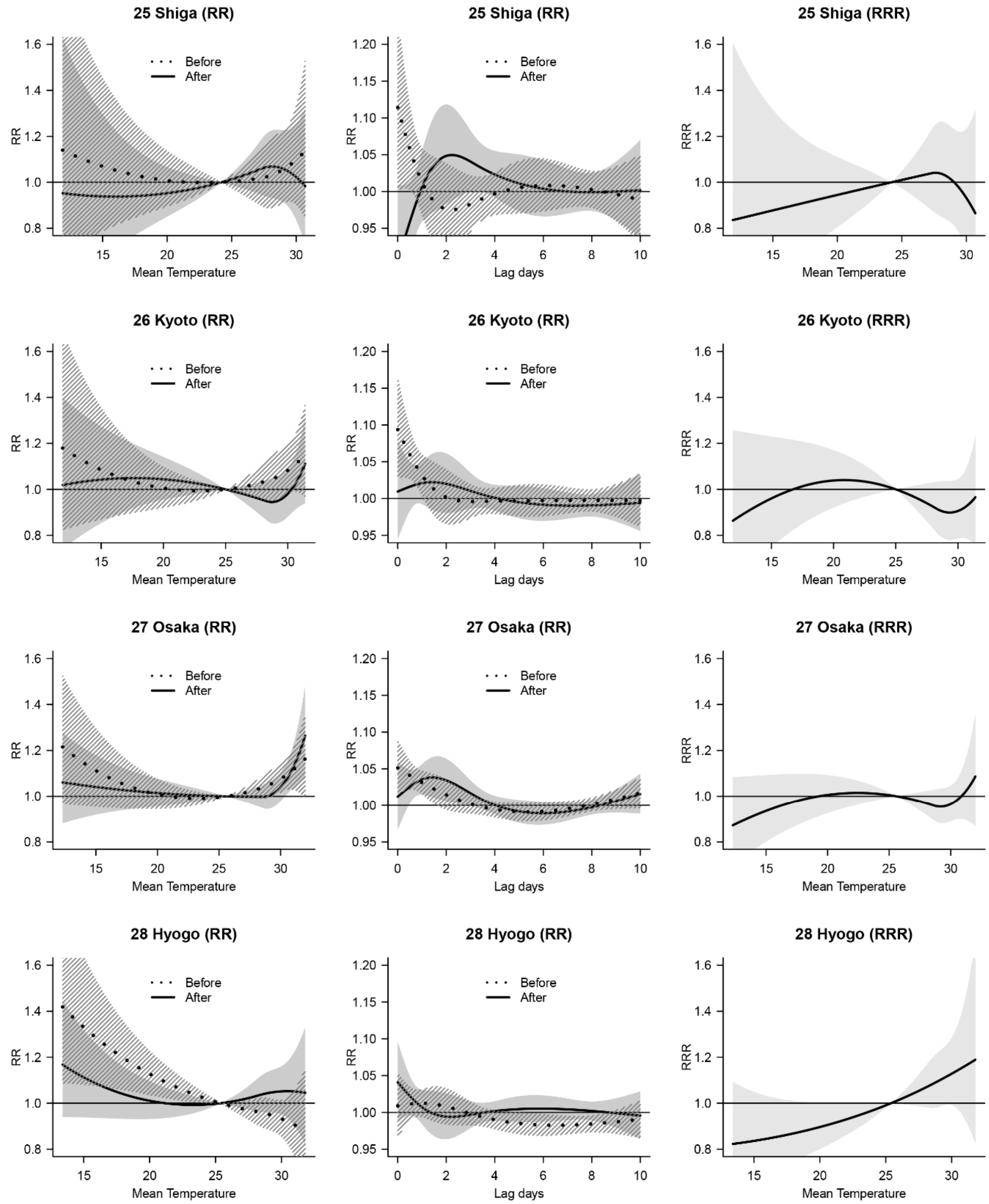

Figure S3. Continued.

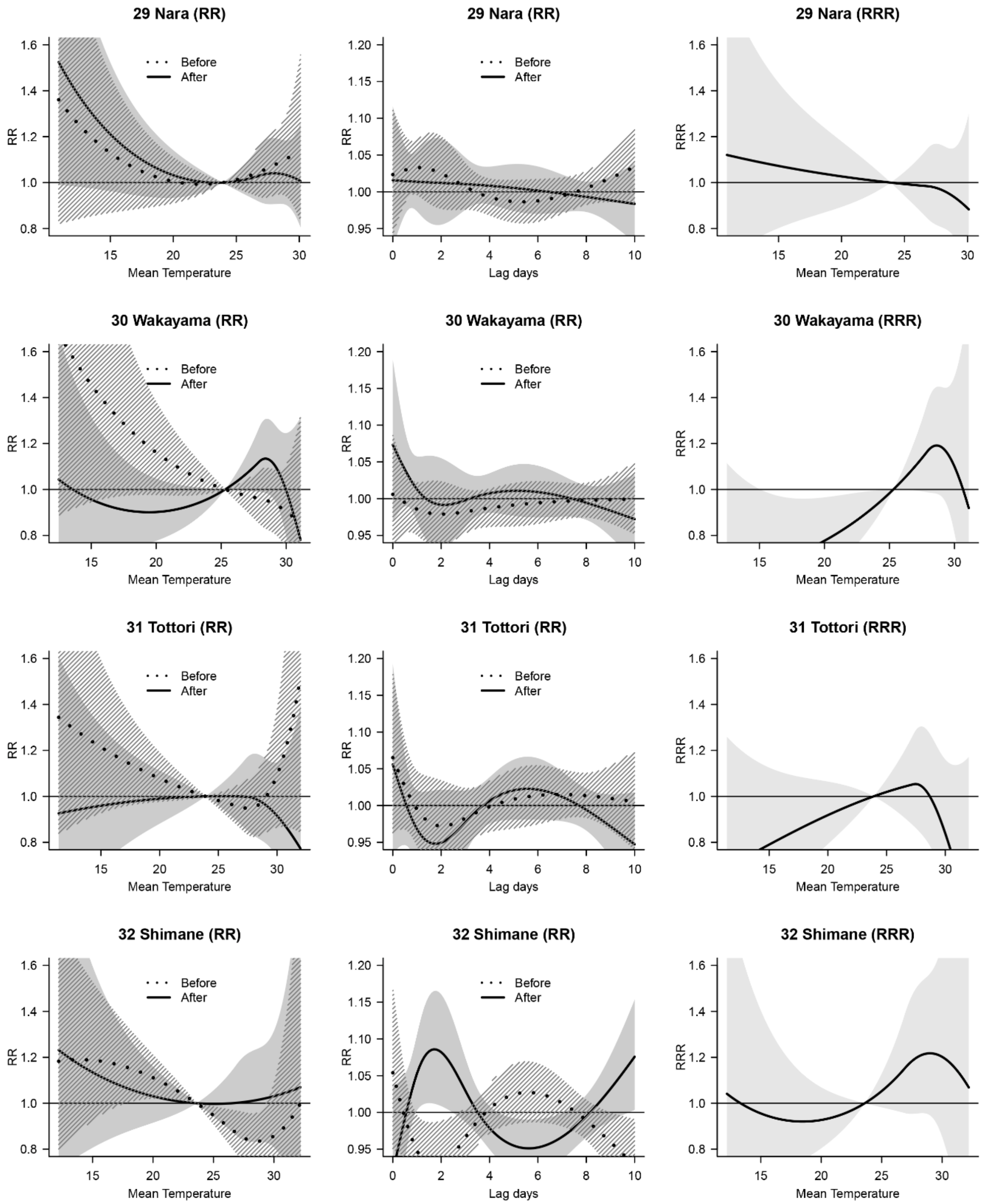

Figure S3. Continued.

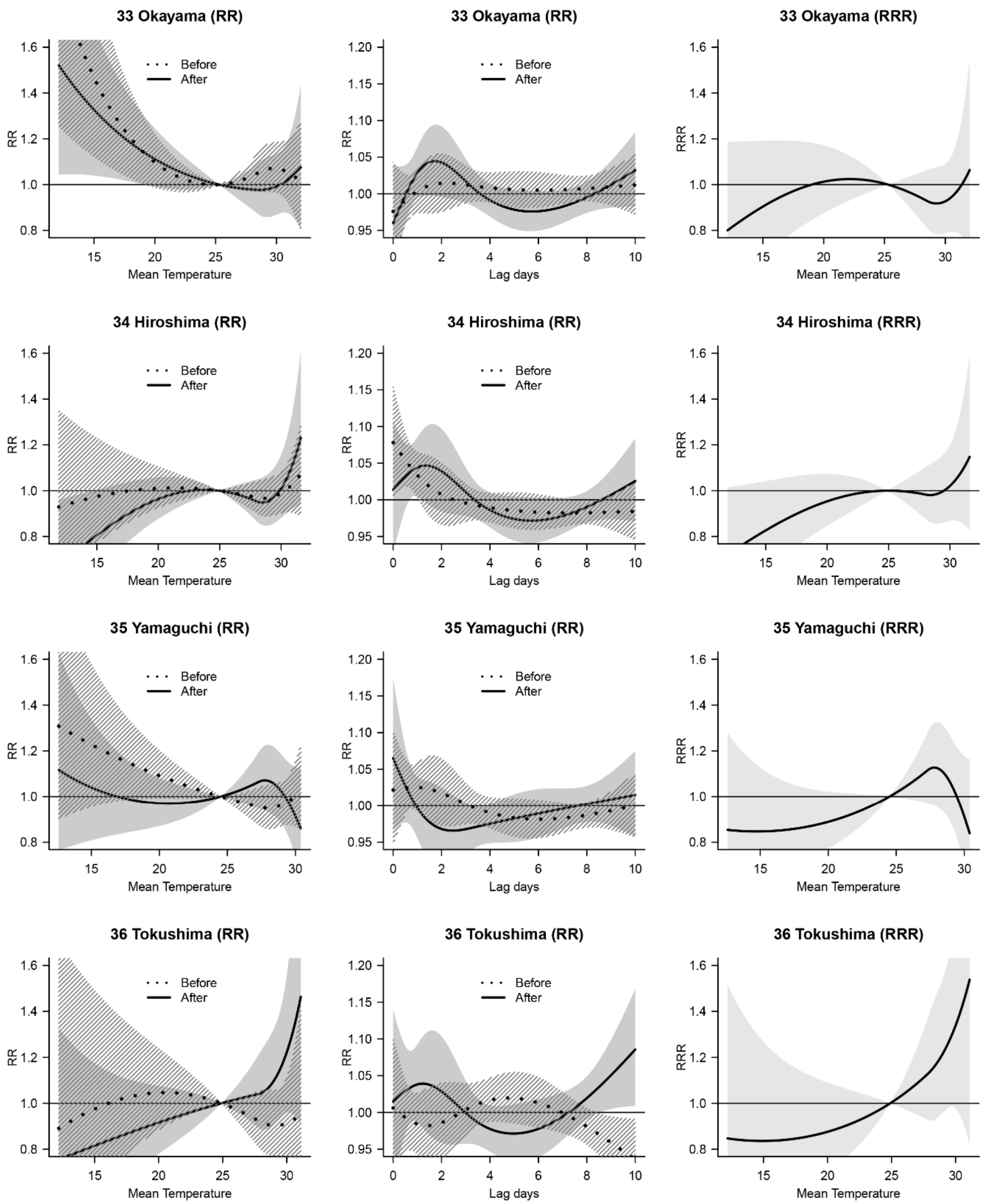

Figure S3. Continued.

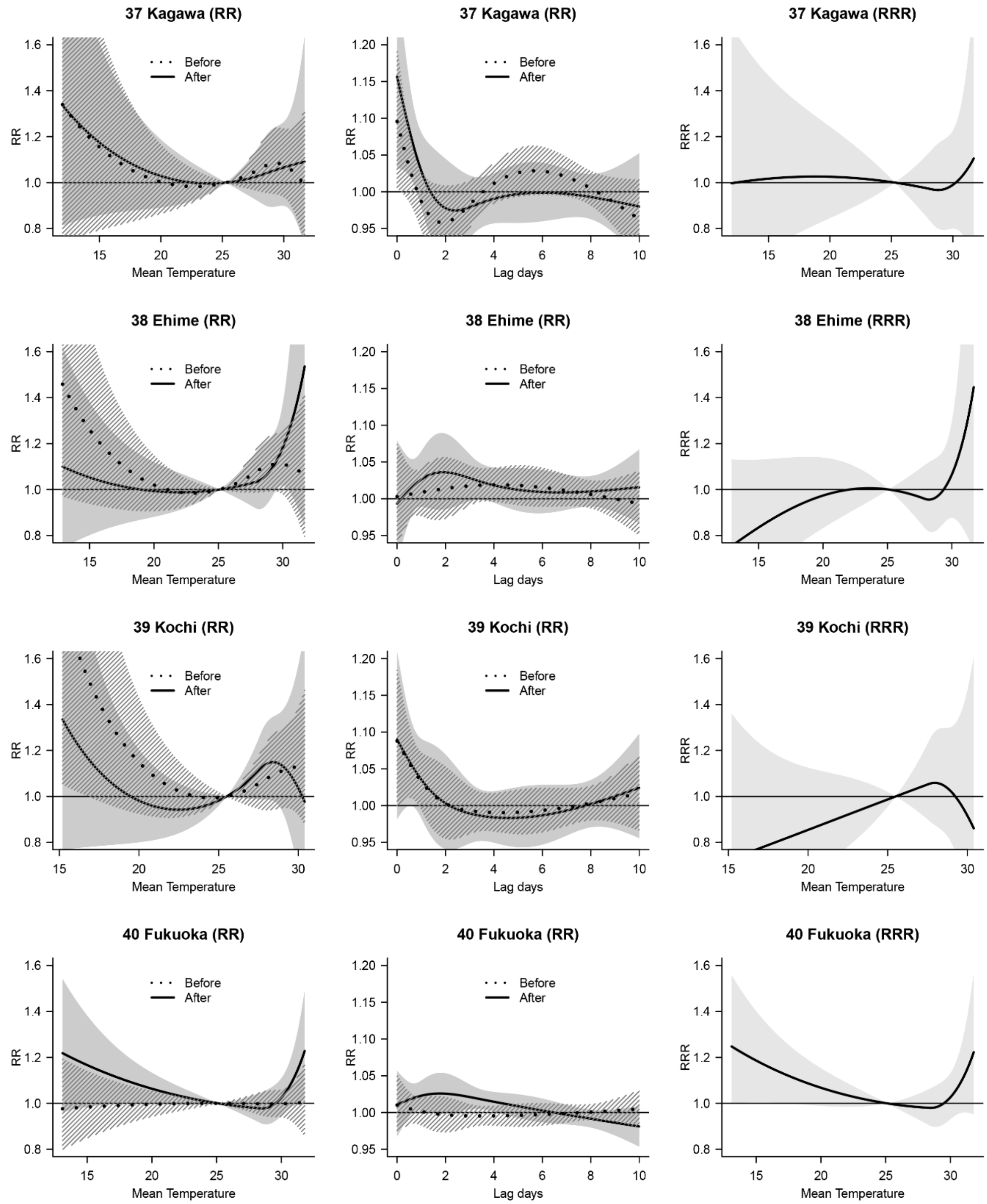

Figure S3. Continued.

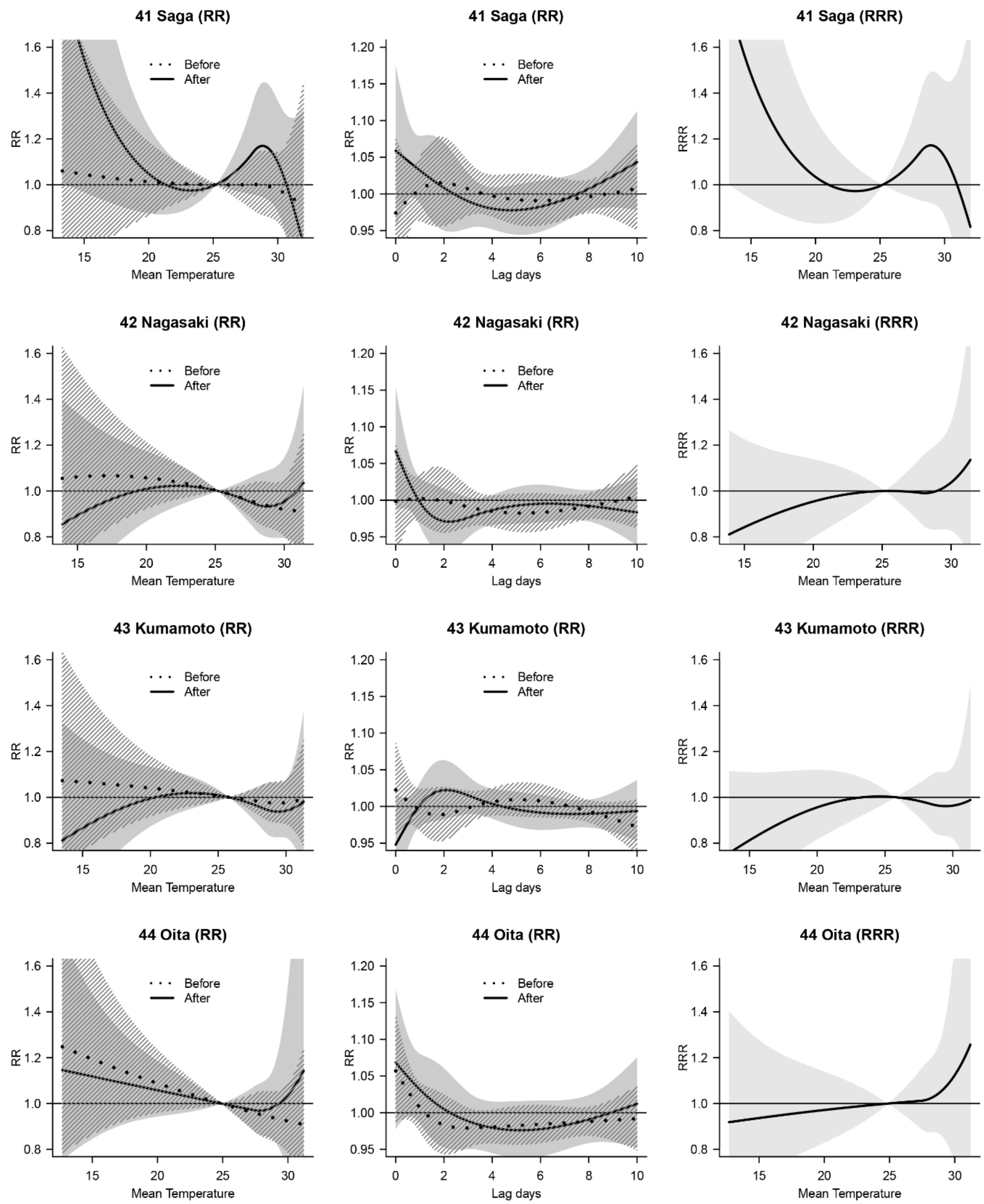

Figure S3. Continued.

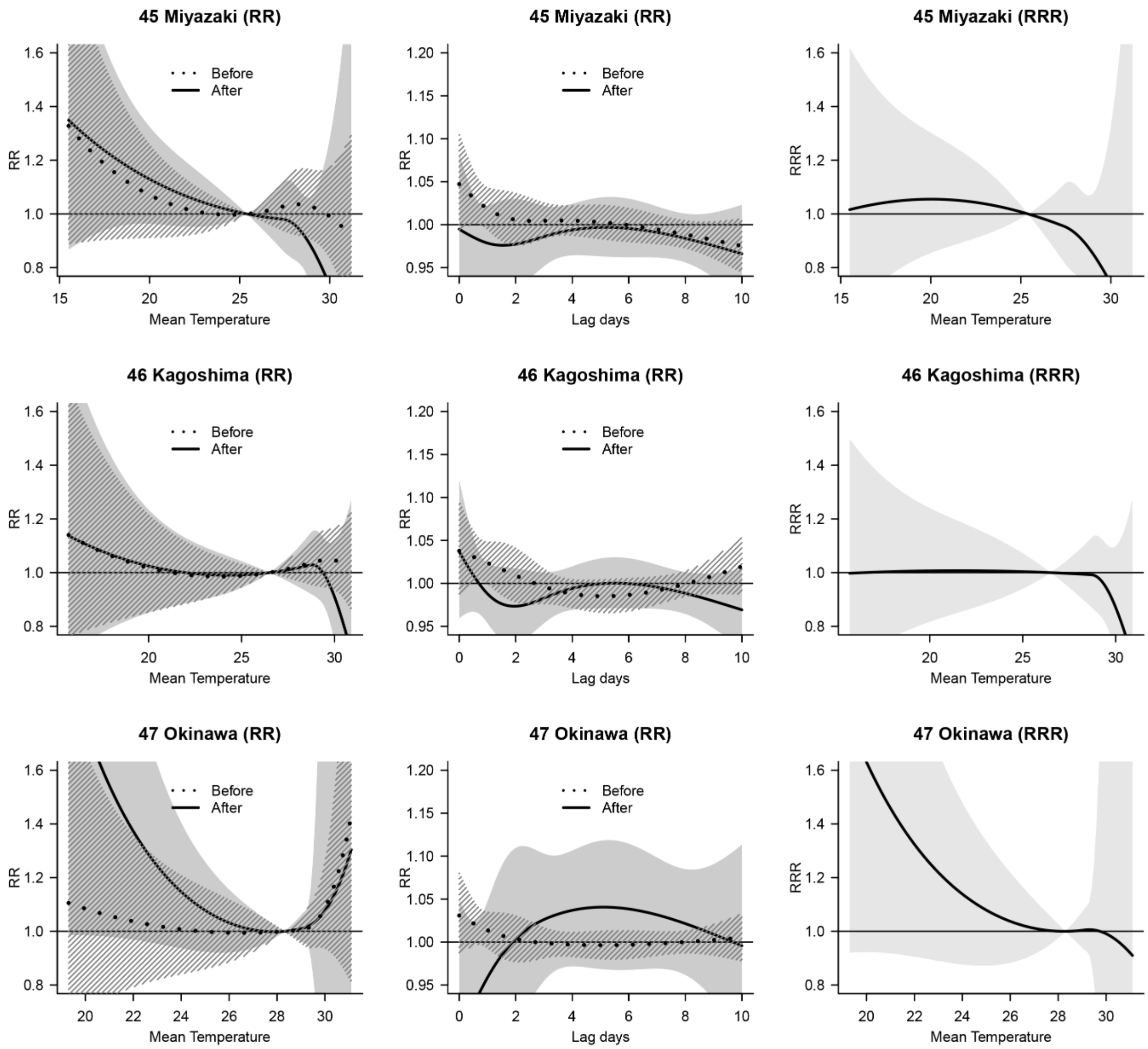

Figure S3. Continued.

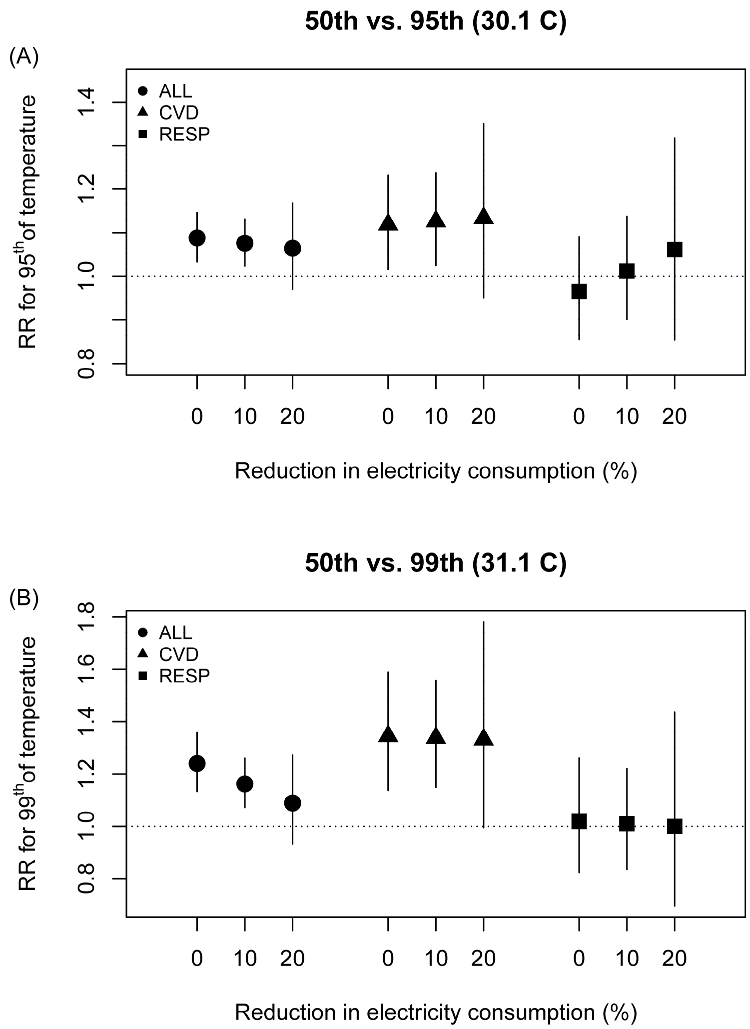

Figure S4. Cumulative relative risks for all-cause (ALL), cardiovascular (CVD), and respiratory (RESP) mortality for people aged 65 and over associated with heat at the 95th (A) or 99th (B) percentiles of daily mean temperature during May–September in Tokyo (30.1°C or 31.1°C, respectively), compared with those for the 50th percentile of the temperature (24.4°C) over 0–10 lag days, stratified by the estimated percent reduction in electricity consumption (i.e. the difference between observed and expected consumption after the earthquake based on a model adjusted for temperature, day-of-week or holiday, and day-in-season using daily electricity consumption in the TEPCO service area that includes Tokyo).

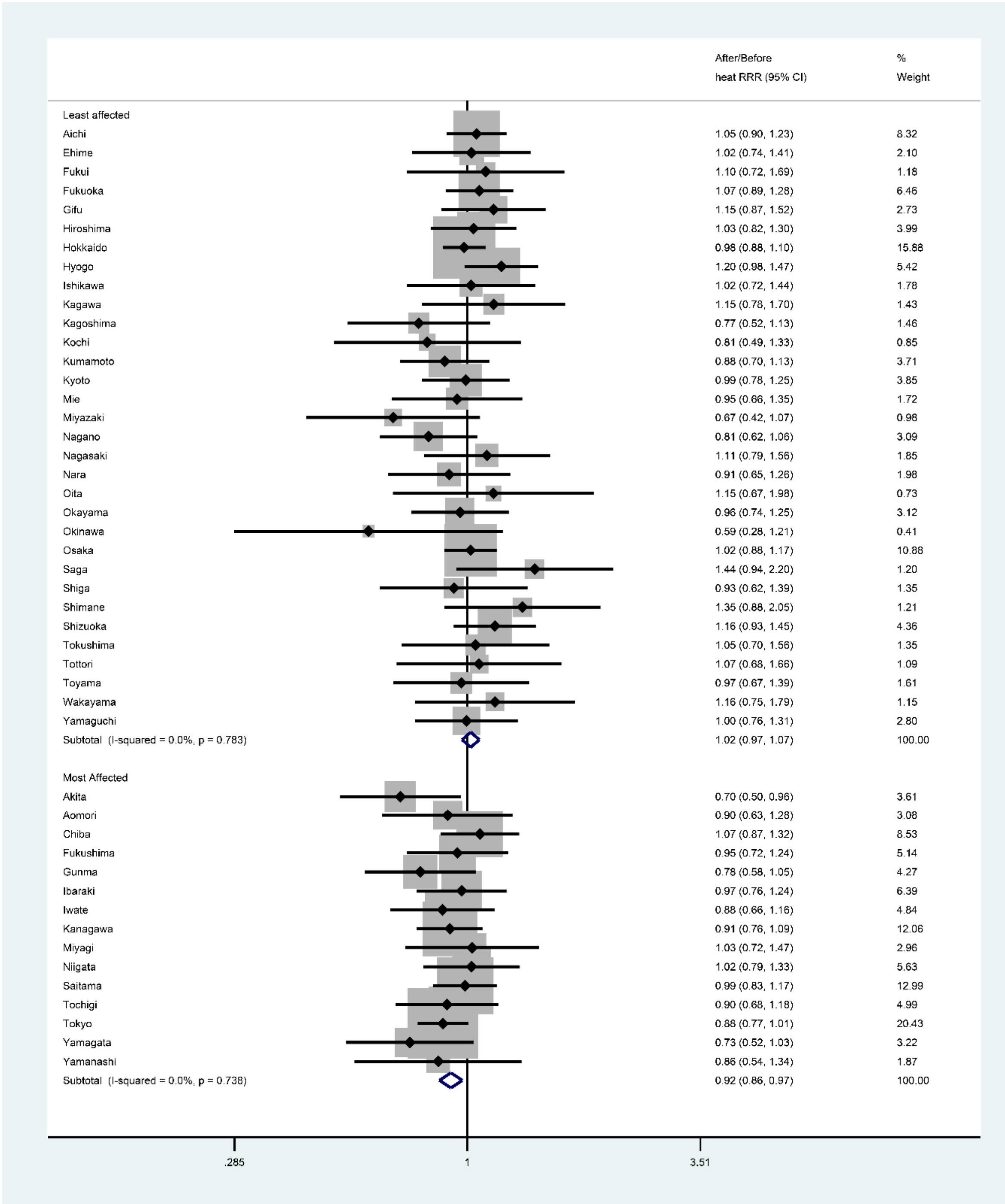

Figure S5. Results by sensitivity analysis excluding the 2011 data showing forest plot for prefecture-specific ratio of relative risks (RRRs) for all-cause mortality associated with heat (the 95th percentile of daily mean temperature during May–September for prefecture specific shown in Table S1) compared with the 50th percentile of the temperature over 0–10 lag days after to before the earthquake and 95% confidence intervals based on the distributed lag non-linear model adjusted for day-of-week or holiday, date, and day-in-season (natural cubic spline with 4 df/year) × year. The periods for before and after correspond to 2008–2010 and 2011–2012, respectively. A fixed effect meta-analysis was used to estimate the summary RRRs in less-affected and most-affected areas. The results were consistent with the main results although the 95% confidence intervals became wider due to the smaller statistical power.

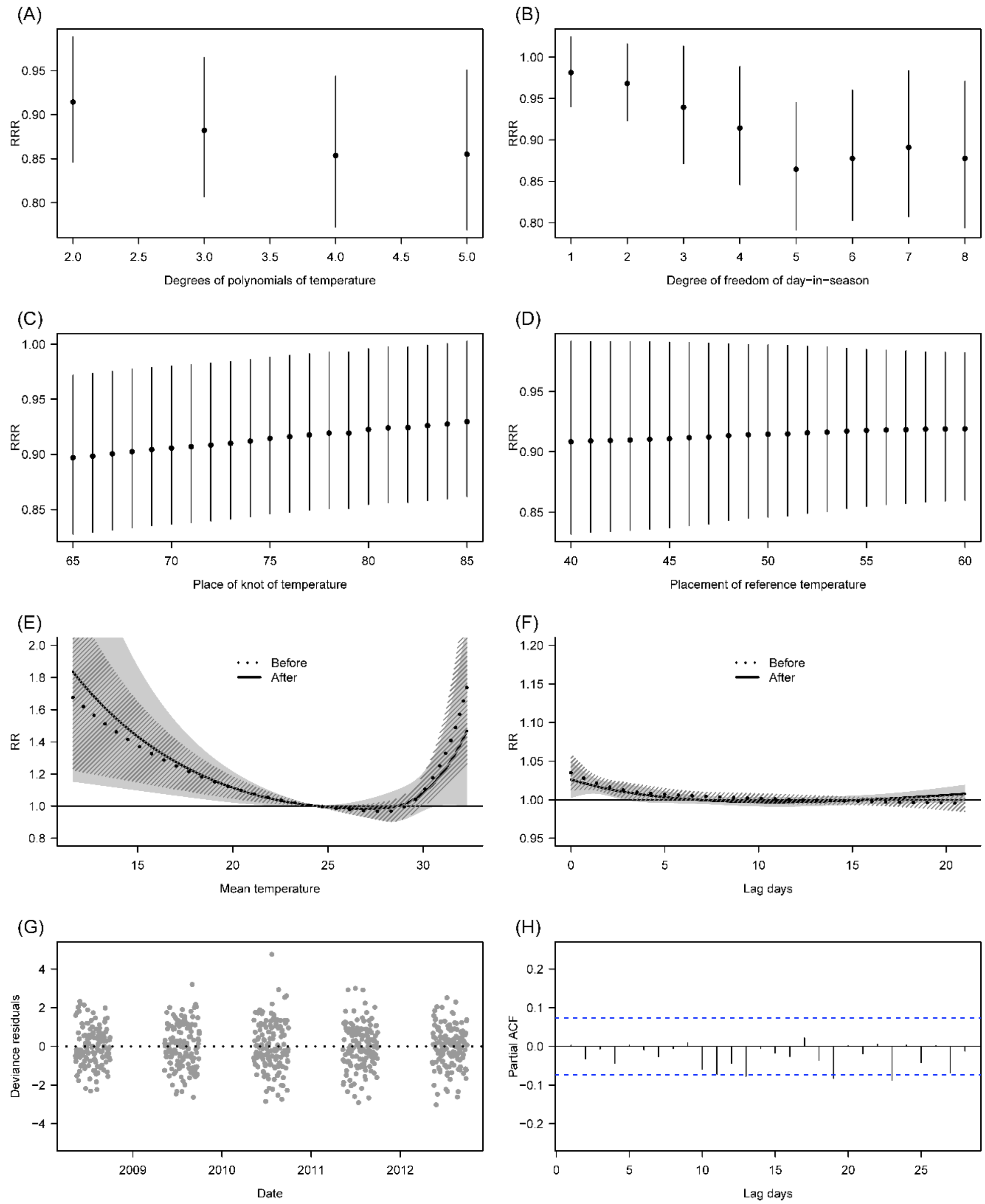

Figure S6. Results by sensitivity analyses. Estimated ratio of relative risks (RRRs) with 95% confidence intervals (CIs) in Tokyo based on the interrupted time-series analysis, according to increases in (A) degree of piecewise polynomials of B-spline basis for temperature, (B) degree of freedom of the natural cubic spline for day-in-season, (C) the place of knot for the spline of temperature, and (D) the placement of reference temperature. (E) The cumulative relative risks for all-cause mortality associated with daily mean temperature during May–September compared with the 50th percentile of the temperature over 0–21 lag days and (F) their lag-response curves for the 95th percentile of daily mean temperature in Tokyo. The shaded areas in panels (E) and (F) indicate 95% confidence intervals. (G) Deviance residuals over time and (H) partial autocorrelation function based on the final model of interrupted time-series analysis in Tokyo.

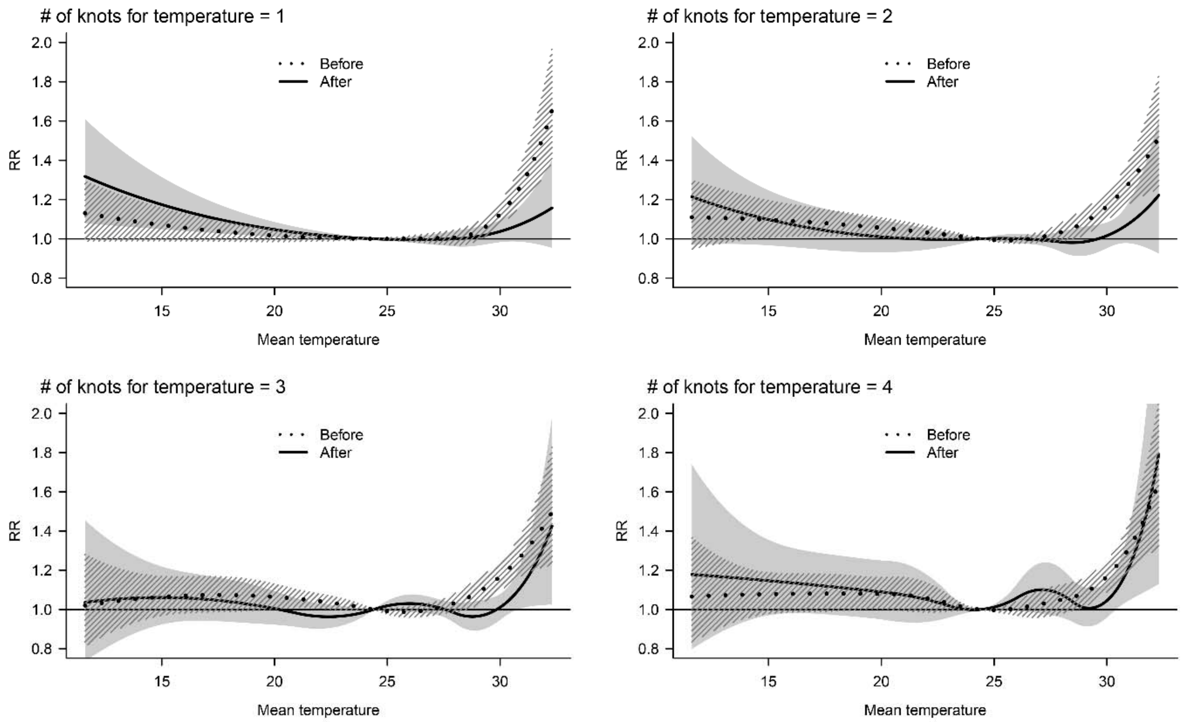

Figure S7. Results by sensitivity analyses. The cumulative relative risks for all-cause mortality associated with daily mean temperature during May–September compared with the 50th percentile of the temperature over 0–10 lag days in Tokyo based on the interrupted time-series analysis, applying a range of number of knots for the quadratic B-spline of daily mean temperature from 1 knot to 4 knots. The shaded areas in each panel indicate 95% confidence intervals.